Supplement of

High-resolution subglacial topography around Dome Fuji, Antarctica, based on ground-based radar surveys conducted over 30 years

Shun Tsutaki et al.

Correspondence to: Shun Tsutaki (tsutaki.shun@nipr.ac.jp)

Table S1. Configurations of VHF radar systems used in this study.

JARE expedition number (period)	Carrier frequency (VHF)	Transmitter pulse width	Numbers of Yagi antenna elements and stacks (for T_x and R_x each)	Antenna gain ($T_x + R_x$)	Vertical resolution	Half-power beamwidth for E-plane	Half-power beamwidth for H-plane
YYYY–YYYY	MHz	ns		dBi	m	degree	degree
26 (1984–1985)	179	300	3 elements × 1	16	26	±35	±45
33 (1992–1993)	179	1000	8 elements × 2	33	85	±20	±10
37 (1996–1997)	60	250	3 elements × 1	14	21	±35	±35
37 (1996–1997)	179	250	3 elements × 1	16	21	±35	±35
40 (1999–2000)	179	250	3 elements × 1	16	21	±35	±35
49 (2007–2008)	179 (POL)	500/60	3 elements × 1 cross	16	42/5	±35	±35
49 (2007–2008)	60	250	3 elements × 1	16	21	±35	±35
54 (2012–2013)	179 (POL)	500/60	3 elements × 1 cross	16	42/5	±35	±35
59 (2017–2018)	179 (POL)	500/100/60	8 elements × 1 cross	27	42/8/5	±20	±22
59 (2017–2018)	179	250/60	11 elements × 2	35	21/5	±15	±5
60 (2018–2019)	179	250/60	16 elements × 2	34	21/5	±15	±5

Table S2. Values of minimum, maximum, mean, absolute mean and standard deviation (σ) of the difference in ice thickness (ΔH) between the JARE gridded data and Bedmap2 (Fretwell et al., 2013), BedMachine Antarctica v1 (Morlighem et al., 2020) and AWI data (Karlsson et al., 2018).

Ice thickness data	Min ΔH	Max ΔH	Mean ΔH	Absolute mean ΔH	σ
	m	m	m	m	m
Bedmap2	−510	812	−33	115	152
BedMachine Antarctica v1	−735	543	−8	83	108
AWI	−515	649	9	121	153

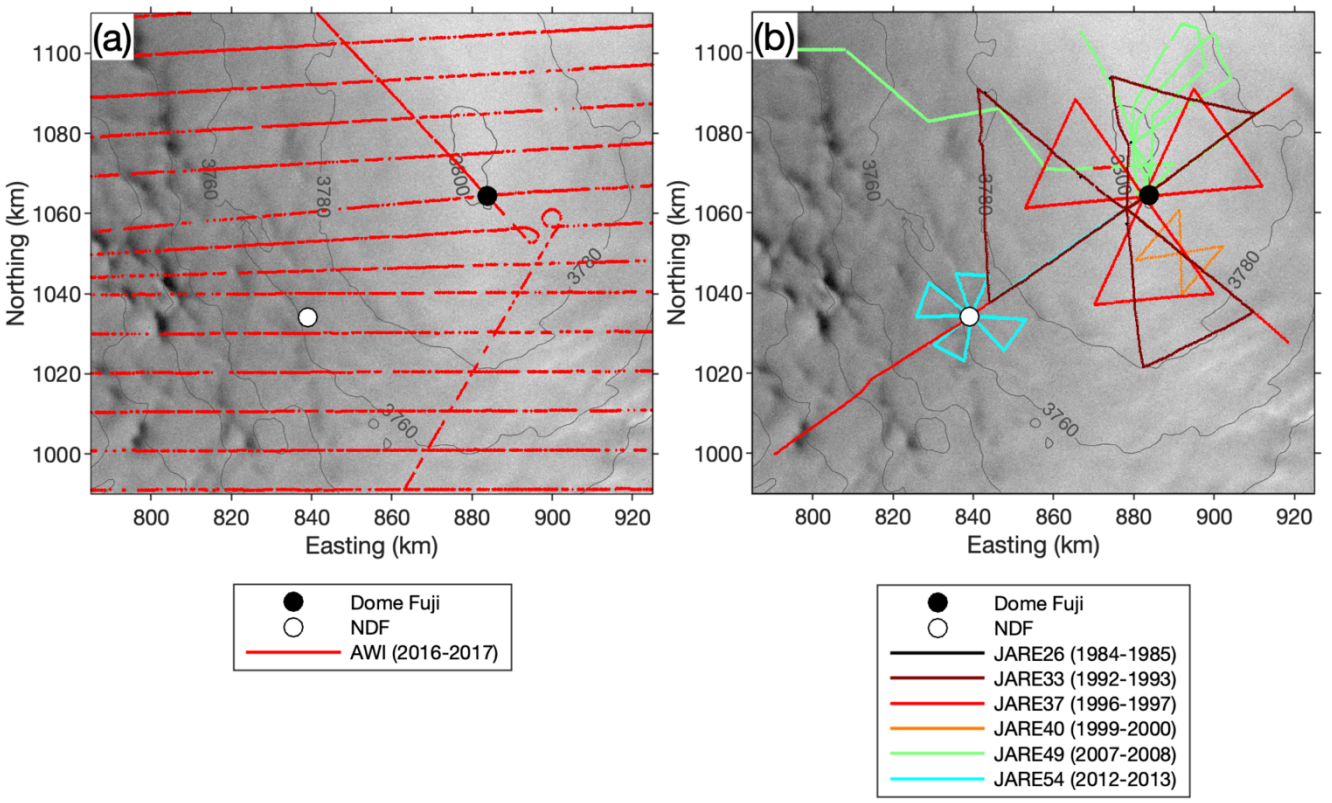

Figure S1. (a) The AWI airborne radar survey lines in the Dome Fuji region (Eisen et al., 2020). Surface elevation contours with intervals of 20 m. Background is RADARSAT-1 image acquired in 1997. (b) The Dome Fuji region showing the coverage of the JARE radar survey lines conducted by radar antennae before modification (JARE26–54). The background is a RADARSAT-1 L1 image (©CSA, 1997).

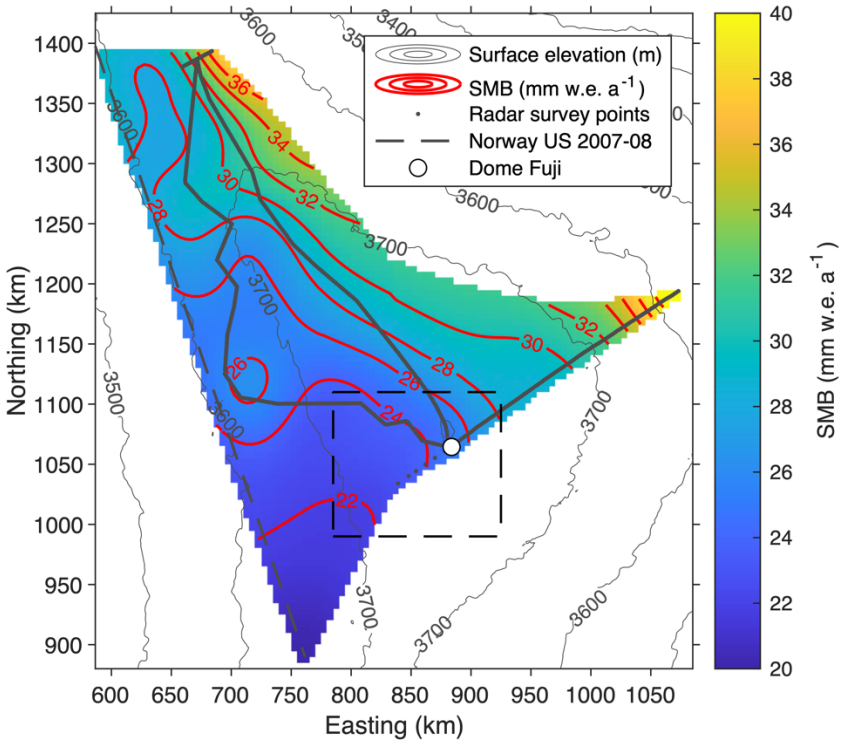

Figure S2. Annual surface mass balance averaged over 722 years, derived from the GPR data compiled by Fujita et al. (2011) and obtained in JARE54. The values were smoothed over 40 km to investigate the large-scale spatial distribution of the surface mass balance in the area. The data were then gridded every 5 km by the spline interpolation scheme for the convenience of presentation. The gray and red contours indicate surface elevation with intervals of 100 m and surface mass balance with intervals of 2 mm w.e. a^{-1}, respectively. The box with black-dashed line indicates the coverage of the ice thickness map constructed in this study.

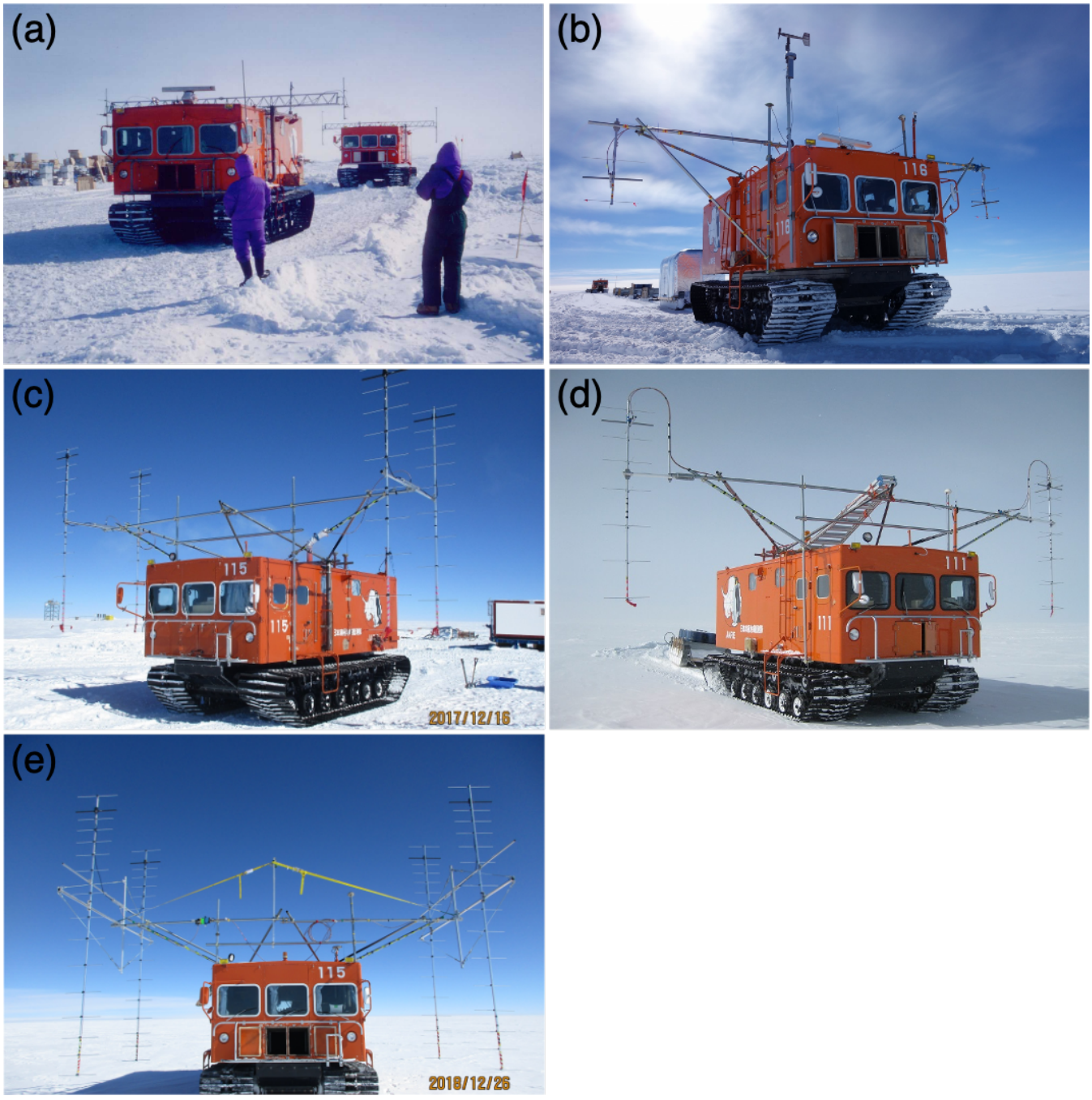

Figure S3. Photographs showing the JARE snow vehicles with various radar antennae. (a) The 60 and 179 MHz VHF pulse modulated radars were set on the vehicles in front and interior, respectively, used in 1996–1997. (b) The 179 MHz VHF radar used in 2012–2013. (c) The 8-element cross antenna and (d) the 11-element antenna used in 2017–2018. (e) The 16-element antenna used in 2018–2019.

References

Eisen, O., Steinhage, D., Karlsson, N. B., Binder, T., and Helm, V.: Ice thickness of the Oldest Ice Reconnaissance survey, 2016/17, Dome Fuji - Beyond EPICA. Alfred Wegener Institute, Helmholtz Centre for Polar and Marine Research, Bremerhaven, PANGAEA, https://doi.org/10.1594/PANGAEA.920234, 2020.

Fretwell, P., Pritchard, H. D., Vaughan, D. G., Bamber, J. L., Barrand, N. E., Bell, R., Bianchi, C., Bingham, R. G., Blankenship, D. D., Casassa, G., Catania, G., Callens, D., Conway, H., Cook, A. J., Corr, H. F. J., Damaske, D., Damm, V, Ferraccioli, F., Forsberg, R., Fujita, S., Gim, Y., Gogineni, P., Griggs, J. A., Hindmarsh, R. C. A., Holmlund, P., Holt, J. W., Jacobel, R. W., Jenkins, A., Jokat, W., Jordan, T., King, E. C., Kohler, J., Krabill, W., Riger-Kusk, M., Langley, K. A., Leitchenkov, G., Leuschen, C., Luyendyk, B. P., Matsuoka, K., Mouginot, J., Nitsche, F. O., Nogi, Y, Nost, O. A., Popov, S. V., Rignot, E., Rippin, D. M., Rivera, A., Roberts, J., Ross, N., Siegert, M. J., Smith, A. M., Steinhage, D., Studinger, M., Sun, B., Tinto, B. K., Welch, B. C., Wilson, D., Young, D. A., Xiangbin, C., and Zirizzotti, A.: Bedmap2: improved ice bed, surface and thickness datasets for Antarctica, The Cryosphere, 7, 375-393, https://doi.org/10.5194/tc-7-375-2013, 2013.

Fujita, S., Holmlund, P., Andersson, I., Brown, I., Enomoto, H., Fujii, Y., Fujita, K., Fukui, K., Furukawa, T., Hansson, M., Hara, K., Hoshina, Y., Igarashi, M., Iizuka, Y., Imura, S., Ingvander, S., Karlin, T., Motoyama, H., Nakazawa, F., Oerter, H., Sjöberg, L. E., Sugiyama, S., Surdyk, S., Ström, J., Uemura, R., and Wilhelms, F.: Spatial and temporal variability of snow accumulation rate on the East Antarctic ice divide between Dome Fuji and EPICA DML, The Cryosphere, 5, 1057–1081, https://doi.org/10.5194/tc-5-1057-2011, 2011.

Karlsson, N. B., Binder, T., Eagles, G., Helm, V., Pattyn, F., Van Liefferinge, B., and Eisen, O.: Glaciological characteristics in the Dome Fuji region and new assessment for "Oldest Ice", The Cryosphere, 12, 2413–2424, https://doi.org/10.5194/tc-12-2413-2018, 2018.

Morlighem, M., Rignot, E., Binder, T., Blankenship, D., Drews, R., Eagles, G., Eisen, O., Ferraccioli, F., Forsberg, R., Fretwell, P., Goel, V., Greenbaum, J. S., Gudmundsson, H., Guo, J., Helm, V., Hofstede, C., Howat, I., Humbert, A., Jokat, W., Karlsson, N. B., Lee, W. S., Matsuoka, K., Millan, R., Mouginot, J., Paden, J., Pattyn, F., Roberts, J., Rosier, S., Ruppel, A., Seroussi, H., Smith, E. C., Steinhage, D., Sun, B., Broeke, M. R. v. d., Ommen, T. D. v., Wessem, M. v., and Young, D. A.: Deep glacial troughs and stabilizing ridges unveiled beneath the margins of the Antarctic ice sheet, Nature Geoscience, 13, https://doi.org/10.1038/s41561-019-0510-8, 2020.